Int. J. Heat Mass Transfer. Vol. 30, No. 10, pp. 1997–2012, 1987
Printed in Great Britain

0017–9310/87 $3.00 + 0.00

Heat transfer in transient buoyancy driven flow adjacent to a horizontal rod

H. M. BADR
Mechanical Engineering Department, University of Petroleum and Minerals, Dhahran, Saudi Arabia

(*Received* 7 *May* 1986 *and in final form* 29 *September* 1986)

Abstract—The problem of heat transfer in transient buoyancy driven flow in the neighbourhood of a horizontal rod of circular cross-section is investigated. The rod, which is placed in a quiescent Boussinesq unbounded fluid, is heated either suddenly or gradually to a constant surface temperature. The investigation is based on the solution of the unsteady two-dimensional conservation equations of mass, momentum and energy in the range of Rayleigh number $10 < Ra < 1000$ while keeping Prandtl number constant at $Pr = 0.7$. Results are presented for the unsteady local and average Nusselt numbers along with some details of the transient temperature and velocity fields. In order to validate the method of solution employed, the steady-state values of average and local Nusselt numbers were also computed and compared with known experimental and theoretical results. The comparison shows a satisfactory agreement.

INTRODUCTION

THE MAIN objective of the present work is to conduct a theoretical investigation to the problem of transient buoyancy driven flow adjacent to a long horizontal rod placed in an infinite Boussinesq fluid. The flow transient occurs due to the change of the rod surface temperature. Transient natural convection problems have received considerable interest for many years, not only because of their fundamental nature but also due to the many related engineering applications ranging from nuclear reactor safety considerations to manufacturing systems where there is a sudden imposition of heat input.

Most of the theoretical studies carried out so far on transient free convection focused on vertical flat and curved surfaces. The works by Goldstein and Briggs [1], Brown and Riley [2], and by Sammakia *et al.* [3] are only a few examples. A good survey of the previous experimental and theoretical studies on these problems is given by Jaluria [4]. In most of these studies the boundary-layer equations were solved by using suitable similarity transformations; a method that may not be appropriate for tackling free convection from bluff bodies such as horizontal cylinders and spheres. Previous theoretical treatment of free convection from horizontal cylinders seem to be delimited to the steady problem rather than the transient one. The works by Merkin [5, 6], Kuehn and Goldstein [7] and by Farouk and Guceri [8] are examples of this.

Only a few theoretical investigations were found in the literature on the problem of transient free convection from a horizontal rod. The first one is that by Elliott [9] who studied the natural convection boundary-layer flow growing over a circular cylinder following a sudden temperature increase from that of the surrounding fluid. The study was based on a series solution at small times for the temperature and stream function. The small time solution was extrapolated to predict the steady value of the heat transfer coefficient. This extrapolation process failed near the top of the cylinder since the boundary-layer approximations were invalid in that region. The approach restricts itself to cases in which the transient free convection flow starts from rest. The boundary-layer approximations cannot be applied for the general case when the initial surface temperature differs from that of the surrounding fluid especially for moderate Grashof numbers. Gupta and Pop [10] studied the effect of curvature on the solution obtained by Elliott [9]. They found that including the curvature effect in the boundary-layer equations leads to an increase in the skin friction as well as the heat rate from the cylinder surface.

Another investigation on this problem was carried out by Ingham [11] who used a Fourier series approximation for the temperature, stream function and vorticity to solve the boundary-layer limit of the governing equations. The solution obtained was only for the case of a sudden temperature rise when Gr is very large. The solution was terminated before reaching the steady conditions, however, comparison with the small time solution obtained by Elliott [9] resulted in a good agreement. The distribution of the local heat transfer at large time was compared with the steady solution of Merkin [5]. The differences were small over all the cylinder surface except near the top where considerable differences were found. These differences were still increasing when the computations were terminated. The local heat rate was continuously decreasing with time in the region of the plume. The adequacy of the boundary-layer solution at low to moderate Rayleigh numbers and also the breakdown of the boundary-layer assumptions, even at large Ray-

NOMENCLATURE

a	rod radius
c	specific heat
f_n	function defined in equation (11)
g	gravitational acceleration
g_n	function defined in equation (11)
Gr	Grashof number, $g\beta(T_s-T_\infty)(2a)^3/\nu^2$
$h, \bar{h}$	local and average heat transfer coefficients
H_0, H_n	functions defined in equation (11)
k	thermal conductivity
$Nu, \overline{Nu}$	local and average Nusselt numbers
Pr	Prandtl number, $\mu c/k$
$\dot{q}$	rate of heat transfer per unit area
r	dimensionless radial coordinate
Ra	Rayleigh number, $Gr\ Pr$
t	dimensionless time
T	temperature
v_r, v_θ	radial and angular velocity components.

Greek symbols

α	thermal diffusivity
β	coefficient of volumetric thermal expansion
ξ	dimensionless logarithmic radial coordinate, $\ln r$
ρ	density
μ	dynamic viscosity
ν	kinematic viscosity
ϕ	dimensionless temperature, $(T-T_\infty)/(T_s-T_\infty)$
ψ	dimensionless stream function, ψ'/α
θ	angular coordinate
ζ	dimensionless vorticity, $\zeta' a^2/\alpha$.

Subscripts

f	final conditions following transient phase
s	rod surface
∞	at infinite distance from the surface.

leigh numbers, in the region of the plume were discussed in refs. [7, 9]. This breakdown occurs mainly because of the thick boundary layer prevailing near the top of the cylinder; a region that is sometimes referred to as the region of colliding or merging boundary layers.

Experimental studies on transient free convection from horizontal cylinders and wires are numerous. Amongst the early studies is the work by Ostroumov [12] who used an optical technique to determine the variation of the thermal field near a horizontal wire following its temperature rise. It was found that the greater the heating electric power used, the sooner the unsteady state ends. The phenomenon of the wire temperature overshoot above its final steady value was observed and related to the delay in the fluid convective motion. The same problem was also investigated by Pera and Gebhart [13] who described the mathematical difficulties in solving such a problem especially in the region near the top of the cylinder where two boundary layers merge forming the buoyant plume. In this region, no flow separation was observed in the experiment.

Vest and Lawson [14] studied the same phenomenon experimentally by visualizing the thermal field around a horizontal wire using a Mach–Zehnder interferometer with emphasis on the delay time between the sudden temperature increase and the beginning of the convective fluid motion. A thermal stability theory was used to predict the time delay which agreed well with the experimental values. More studies on the same problem were carried out by Parsons and Mulligan [15]. In their work, an overshoot of the steady state was observed during the transient decay of the average Nusselt number. The transient period was shown to be divided into three distinct stages which are, pure conduction, convective transition, and finally steady free convection. The relationship between the occurrence of the overshoot and Rayleigh number was also discussed. In another study [16], the same authors extended their investigation to the case of a horizontal cylinder of finite (not very small) diameter with emphasis on the application of the thermal stability theory used in refs. [14, 15] to high Rayleigh numbers. Recently, the transition from conduction to convection around horizontal wires in the case of a ramp excursion in internal heat generation was studied by Faw *et al.* [17]. They found that the transition time depends on the rate of increase of heat generation and is independent of the wire diameter. Transition time was measured up to Rayleigh number $Ra = 31$.

In this work, the problem of transient buoyancy driven flow adjacent to a horizontal rod of circular cross-section placed in an unbounded fluid is investigated in the range of Rayleigh number $10 < Ra < 1000$ while Prandtl number is kept constant. The flow transient occurs due to either sudden or gradual increase in the rod surface temperature. The study is based on the solution of the conservation equations of mass, momentum and energy. Results are presented in the form of the variation of the average Nusselt number as well as the developing streamlines and isotherms during the transient phase. The overshoot phenomenon which occurred in several cases is discussed in some detail.

PROBLEM STATEMENT AND GOVERNING EQUATIONS

The problem considered is that of a long horizontal rod of a circular cross-section placed in a quiescent fluid of infinite extent. The rod and the fluid have an initial temperature T_∞. The temperature of the rod surface is either gradually or suddenly increased to T_{sf}. A buoyancy driven flow starts near the rod surface and develops with time until reaching the final steady condition. The rod is considered to be long enough such that the end effects can be neglected and the flow can be assumed two-dimensional. The viscous dissipation is neglected and the temperature difference is assumed to have a negligible effect on the fluid properties except for the density in the buoyancy force term in the momentum equation.

Consider the line $\theta = 0$ to be the vertical line through the center O of the rod cross-section as shown in Fig. 1. Using a cylindrical coordinate system, the equations of motion and energy can be written in terms of the stream function ψ', vorticity ζ', and temperature T as

$$\frac{\partial \zeta'}{\partial t'} + \frac{1}{r'}\frac{\partial \psi'}{\partial \theta}\frac{\partial \zeta'}{\partial r'} - \frac{1}{r'}\frac{\partial \psi'}{\partial r'}\frac{\partial \zeta'}{\partial \theta} = \nu \nabla^2 \zeta + \frac{1}{\rho}\left[\frac{\partial F_\theta}{\partial r'} - \frac{1}{r'}\frac{\partial F_r}{\partial \theta} + \frac{F_\theta}{r'}\right] \quad (1)$$

$$\zeta' = -\nabla^2 \psi' \quad (2)$$

$$\frac{\partial T}{\partial t'} + \frac{1}{r'}\frac{\partial \psi'}{\partial \theta}\frac{\partial T}{\partial r'} - \frac{1}{r'}\frac{\partial \psi'}{\partial r'}\frac{\partial T}{\partial \theta} = \frac{k}{\rho c}\nabla^2 T \quad (3)$$

where

$$\nabla^2 = \frac{\partial^2}{\partial r'^2} + \frac{1}{r'}\frac{\partial}{\partial r'} + \frac{1}{r'^2}\frac{\partial^2}{\partial \theta^2}$$

t' is the time, ρ the density, ν the kinematic viscosity, k the fluid thermal conductivity and c the specific heat. $F_{r'}$ and F_θ are the radial and angular components of the buoyancy force and are defined as

$$F_{r'} = \rho g \beta (T - T_\infty)\cos\theta$$

$$F_\theta = -\rho g \beta (T - T_\infty)\sin\theta$$

where g is the gravitational acceleration and β is the coefficient of volumetric thermal expansion. The velocity components v_r' and v_θ' are related to ψ' by

$$v_r' = 1/r'\,\partial\psi'/\partial\theta \quad \text{and} \quad v_\theta' = -\partial\psi'/\partial r'.$$

The following dimensionless quantities are now introduced

$$\psi = \psi'/\alpha, \quad \zeta = -\zeta' a^2/\alpha, \quad r = r'/a,$$
$$t = t'\alpha/a^2, \quad V_r = v_r' a/\alpha, \quad v_\theta = v_\theta' a/\alpha$$

and

$$\phi = (T - T_\infty)/(T_s - T_\infty)$$

where $\alpha = k/\rho c$ is the thermal diffusivity. Using the above variables in equations (1)–(3) results in

$$\frac{\partial \zeta}{\partial t} + \frac{1}{r}\frac{\partial \psi}{\partial \theta}\frac{\partial \zeta}{\partial r} - \frac{1}{r}\frac{\partial \psi}{\partial r}\frac{\partial \zeta}{\partial \theta} = Pr\,\nabla^2 \zeta + \frac{Gr\,Pr^2}{8}\left[\frac{\partial \phi}{\partial r}\sin\theta + \frac{1}{r}\frac{\partial \phi}{\partial \theta}\cos\theta\right] \quad (4)$$

$$\zeta = \nabla^2 \psi \quad (5)$$

$$\frac{\partial \phi}{\partial t} + \frac{1}{r}\frac{\partial \psi}{\partial \theta}\frac{\partial \phi}{\partial r} - \frac{1}{r}\frac{\partial \psi}{\partial r}\frac{\partial \phi}{\partial \theta} = \nabla^2 \phi - \frac{\phi}{Ra}\frac{\partial Ra}{\partial t} \quad (6)$$

where $Pr = \nu/\alpha$ is the Prandtl number, $Gr = g\beta(T_s - T_\infty)(2a)^3/\nu^2$ the Grashof number, and $Ra = Gr\,Pr$ the Rayleigh number. The dimensionless velocity components v_r and v_θ are now defined as

$$v_r = 1/r\,\partial\psi/\partial\theta \quad \text{and} \quad v_\theta = -\partial\psi/\partial r.$$

The boundary conditions for ψ, ζ and ϕ are based on the no-slip, impermeability and isothermal conditions on the rod surface and the ambient conditions far away from it. These conditions can be expressed as

$$1/r\,\partial\psi/\partial\theta = \partial\psi/\partial r = 0, \phi = 1 \quad \text{at} \quad r = 1$$

and

$$1/r\,\partial\psi/\partial\theta, \partial\psi/\partial r, \phi, \zeta \to 0 \quad \text{as} \quad r \to \infty.$$

The conditions on the line of symmetry $\theta = 0$ and π can be expressed as

$$v_\theta = \partial v_r/\partial\theta = \zeta = \partial\phi/\partial\theta = 0.$$

In order to achieve a highly accurate numerical solution, the logarithmic radial coordinate ξ is used such that $\xi = \ln r$ which transforms the governing equations (4)–(6) to

$$e^{2\xi}\frac{\partial \zeta}{\partial t} = Pr\left(\frac{\partial^2 \zeta}{\partial \xi^2} + \frac{\partial^2 \zeta}{\partial \theta^2}\right) - \frac{\partial \psi}{\partial \theta}\frac{\partial \zeta}{\partial \xi} + \frac{\partial \psi}{\partial \xi}\frac{\partial \zeta}{\partial \theta} + \frac{1}{8}e^{\xi}\,Gr\,Pr^2\left[\frac{\partial \phi}{\partial \xi}\sin\theta + \frac{\partial \phi}{\partial \theta}\cos\theta\right] \quad (7)$$

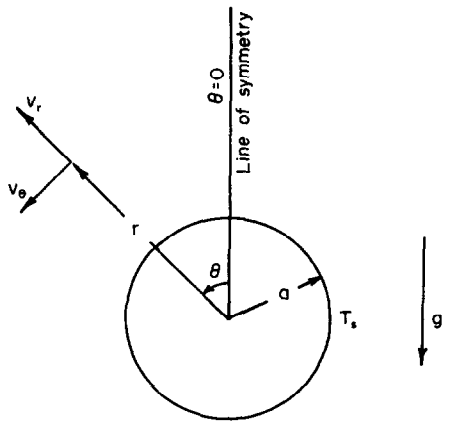

FIG. 1. Coordinate system.

$$e^{2\xi}\zeta = \frac{\partial^2\psi}{\partial\xi^2} + \frac{\partial^2\psi}{\partial\theta^2} \quad (8)$$

$$e^{2\xi}\left[\frac{\partial\phi}{\partial t} + \frac{\phi}{Ra}\frac{\partial Ra}{\partial t}\right] = \frac{\partial^2\phi}{\partial\xi^2} + \frac{\partial^2\phi}{\partial\theta^2} - \frac{\partial\psi}{\partial\theta}\frac{\partial\phi}{\partial\xi} + \frac{\partial\psi}{\partial\xi}\frac{\partial\phi}{\partial\theta}. \quad (9)$$

It is important to mention that the term $\partial Ra/\partial t$ in equation (9) has a non-zero value in the case when the rod surface temperature increases gradually. However, in the case of a sudden temperature increase $\partial Ra/\partial t = 0$ immediately following the temperature rise.

In terms of the new variables, the boundary conditions can be written as

$$\psi = \partial\psi/\partial\xi = \partial\psi/\partial\theta = 0, \phi = 1 \quad \text{at} \quad \xi = 0,$$
$$e^{-\xi}\,\partial\psi/\partial\theta, e^{-\xi}\,\partial\psi/\partial\xi, \phi, \zeta \to 0 \quad \text{as} \quad \xi \to \infty \quad (10)$$

and Ra is either a constant or a known function of time.

THE NUMERICAL SOLUTION

The method used for solving the unsteady equations (7)–(9) to obtain the time development of the velocity and temperature distributions in the flow field is based on approximating ψ, ζ and ϕ in terms of a truncated Fourier series following the work done by Collins and Dennis [18], Badr and Dennis [19] and Badr [20]. In the present study, the rod surface which was initially at temperature T_∞, is heated in a certain prescribed form such that T_s is a known function of time. During and following this temperature change, a buoyancy driven flow starts near the rod and develops with time.

For all forms of heating and provided that the rod surface has a uniform temperature distribution, the velocity and temperature fields are symmetric about the vertical radius ($\theta = 0$). Following ref. [20], ψ, ζ and ϕ can be expressed as

$$\psi = \sum_{n=1}^{N} f_n(\xi, t)\sin n\theta$$
$$\zeta = \sum_{n=1}^{N} g_n(\xi, t)\sin n\theta \quad (11)$$
$$\phi = \frac{1}{2}H_0(\xi, t) + \sum_{n=1}^{N} H_n(\xi, t)\cos n\theta.$$

The use of equation (11) with equations (7)–(9) results in the following sets of equations to be solved for the functions f_n, g_n, H_0 and H_n

$$\frac{\partial^2 f_n}{\partial\xi^2} - n^2 f_n = e^{2\xi} g_n \quad (12)$$

$$2e^{2\xi}\frac{\partial g_n}{\partial t} = 2Pr\left(\frac{\partial^2 g_n}{\partial\xi^2} - n^2 g_n\right) + S_n(\xi, t) \quad (13)$$

$$e^{2\xi}\frac{\partial H_0}{\partial t} = \frac{\partial^2 H_0}{\partial\xi^2} - \frac{1}{Ra}e^{2\xi}\frac{\partial Ra}{\partial t}H_0 + Z_0(\xi, t) \quad (14)$$

$$2e^{2\xi}\frac{\partial H_n}{\partial t} = 2\left[\frac{\partial^2 H_n}{\partial\xi^2} - n^2 H_n\right] - nf_n\frac{\partial H_0}{\partial\xi} - \frac{2}{Ra}e^{2\xi}\frac{\partial Ra}{\partial t}H_n + Z_n(\xi, t) \quad (15)$$

where the terms S_n, Z_0 and Z_n are easily identifiable functions of ξ and t. The boundary conditions for all the above functions are deduced from equation (10) and can be expressed as

$$f_n = H_n = \partial f_n/\partial\xi = 0 \quad \text{and} \quad H_0 = 2 \quad \text{at} \quad \xi = 0$$
$$g_n, H_0, H_n, \partial f_n/\partial\xi \to 0 \quad \text{as} \quad \xi \to \infty. \quad (16)$$

The following integral condition is obtained by integrating both sides of equation (12) with respect to ξ between $\xi = 0$ and ∞ and using the conditions given in equation (16)

$$\int_0^\infty e^{(2-n)\xi} g_n(\xi, t)\,d\xi = 0. \quad (17)$$

Although the differential equations (12)–(15) and the boundary and integral conditions are different from those deduced in ref. [20] to study the problem of laminar mixed convection from a horizontal cylinder, the numerical procedure used in this work is almost the same and therefore will not be discussed again.

DISCUSSION OF RESULTS

The behaviour of the velocity and thermal fields near the horizontal rod during and following its temperature increase from T_∞ to T_{sf} is studied for moderate Rayleigh numbers ($10 < Ra < 1000$). Since the problem of a step temperature increase has been of major interest in many experimental investigations, it is considered here and this mode of heating is referred to as the first mode. However, a sudden change of temperature is unusual and may be unrealistic in practical applications because it requires a body of infinitely small thermal capacity in addition to a step change in the input heat. A gradual temperature increase is of major interest in engineering applications, although it has not received, so far, much attention either theoretically or experimentally. In this work, the transient phenomenon is investigated when the temperature increase is gradual. The simplest case is when the temperature increases linearly with time from T_∞ to T_{sf} during a time period t_f and this mode is referred to as the second mode. In this mode the term $\partial\phi/\partial t$ in the energy equation has discontinuities at $t = 0$ and t_f. In the third mode, the temperature–time curve is a smooth one which is likely to be the case of practical interest. The relation between T_s and t is considered in the simple form

$$\frac{T_s - T_\infty}{T_{sf} - T_\infty} = 2\frac{t}{t_f} - \left(\frac{t}{t_f}\right)^2. \quad (18)$$

The three modes of heating are presented graphically in Fig. 2.

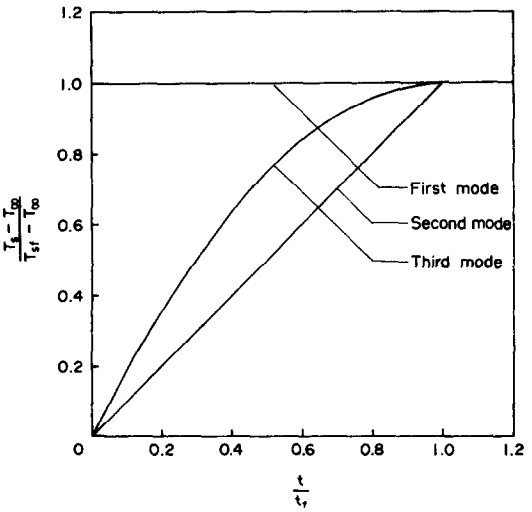

FIG. 2. Surface temperature change for the three modes of heating.

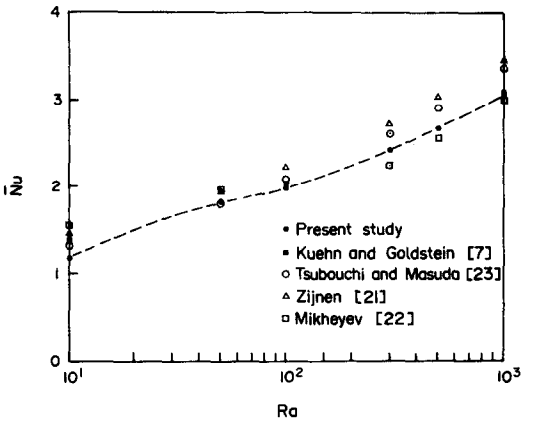

FIG. 3. Comparison of the steady values of the average Nusselt number with previous theoretical and experimental results.

The local and average Nusselt numbers Nu and $\overline{Nu}$ are defined such that

$$Nu = 2ah/k \quad \text{and} \quad \overline{Nu} = 2a\bar{h}/k \tag{19}$$

where k is the coefficient of thermal conductivity and h and $\bar{h}$ are the local and average heat transfer coefficients defined as

$$h = \dot{q}/(T_{sf} - T_\infty), \quad \bar{h} = (1/2\pi)\int_0^{2\pi} h \, d\theta \tag{20}$$

where $\dot{q}$ is the rate of heat transfer per unit area given by

$$\dot{q} = -k(\partial T/\partial r')_{r'=a}. \tag{21}$$

Using the dimensionless temperature ϕ together with the above definitions, one can easily deduce

$$Nu = -2[\partial\phi/\partial\xi]_{\xi=0} Ra/Ra_f \tag{22a}$$

and

$$\overline{Nu} = [-\partial H_0/\partial\xi]_{\xi=0} Ra/Ra_f \tag{22b}$$

where Ra_f is the final steady value of the Rayleigh number [based on $(T_{sf} - T_\infty)$].

In order to verify the accuracy of the method of solution and the numerical computations, the final steady values of $\overline{Nu}$ were compared with the available experimental and theoretical data as can be seen in Fig. 3. The figure shows a small difference between the present results and those obtained by Kuehn and Goldstein [7] over most of the considered range of Ra. The difference between the two is 2.2% at $Ra = 1000$, however at $Ra = 10$ the difference reaches 14%. In ref. [7], the flow is assumed to approach the cylinder radially and is also assumed to leave radially in the plume with negligible radial temperature gradient. No such assumptions are made in the present study. The comparison with the experimental correlations given in refs. [21–23] as shown in Fig. 3 indicate a deviation as high as 18%, however, a difference of the same order occurs between these correlations which can be due to inaccuracies in the measurements. Figure 4 shows the steady local Nusselt number distribution on the rod surface for $Ra = 100$ and 1000 together with the results given in ref. [7] for comparison.

The transient decay of $\overline{Nu}$ following a sudden temperature rise is proved to be exactly the same as that for the transient conduction problem at small times [12, 14, 15] because of the small velocities prevailing in the immediate neighbourhood of the rod surface. It was also found experimentally that the convective motion in this mode of heating is delayed for a certain period of time [16, 17]. This criterion has been used to check the accuracy of the small time solution obtained in the present work. Figure 5 shows a comparison

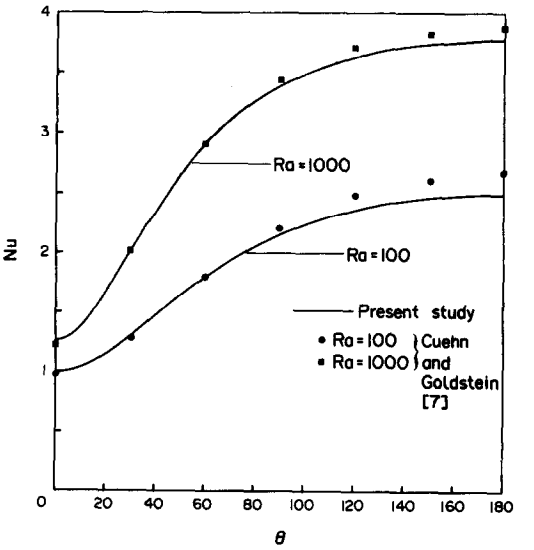

FIG. 4. Comparison of the steady local Nusselt number distribution with previous results for $Ra = 100$ and 1000.

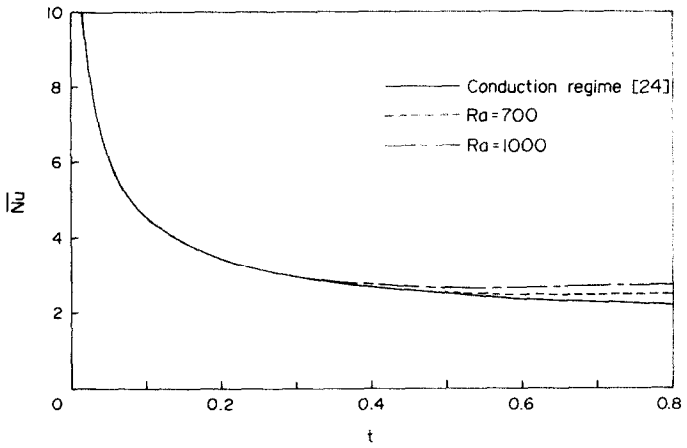

FIG. 5. Comparison of the small time results with the analytical solution of the conduction problem.

between the variation of $\overline{Nu}$ when $Ra = 700$ and 1000 with the solution of the conduction problem as given in ref. [24]. The figure shows an excellent agreement at small times, however, the two curves deviate at large times due to the convective motion near the rod surface.

Figure 6 shows the variation of $\overline{Nu}$ following sudden temperature rise from T_∞ to T_{sf} until reaching steady conditions. It is clear from the figure that the time required to reach the final steady value of $\overline{Nu}$ decreases as Ra increases. This can be explained on the basis that increasing Ra tends to increase the buoyancy force accelerating the flow near the rod surface and accordingly decreasing the time delay until the start of the convective fluid motion. Following this motion the value of $\overline{Nu}$ increases above that of the corresponding conduction regime causing the known phenomenon of heat transfer overshoot. This phenomenon is clearly shown in Fig. 6 especially for $Ra > 100$, however, no significant overshoot occurs for the cases of $Ra = 10$ and 50. With the increase of Ra, this phenomenon occurs earlier and becomes more pronounced as expected. The same behaviour was found experimentally and reported in refs. [14–17] with emphasis on the delay time until the transition from conduction to convection dominated regime takes place.

The variation of $\overline{Nu}$ with time for the second and third modes of heating are shown in Figs. 7 and 8 for the case of $R = 100$ and at various rates of tem-

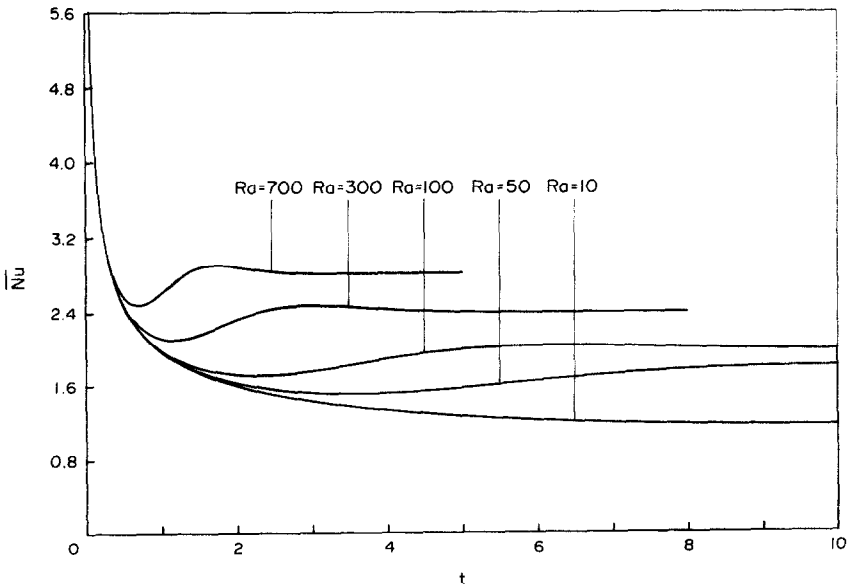

FIG. 6. The variation of the average Nusselt number for the first mode—cases of $Ra = 10$, 50, 100, 300 and 700.

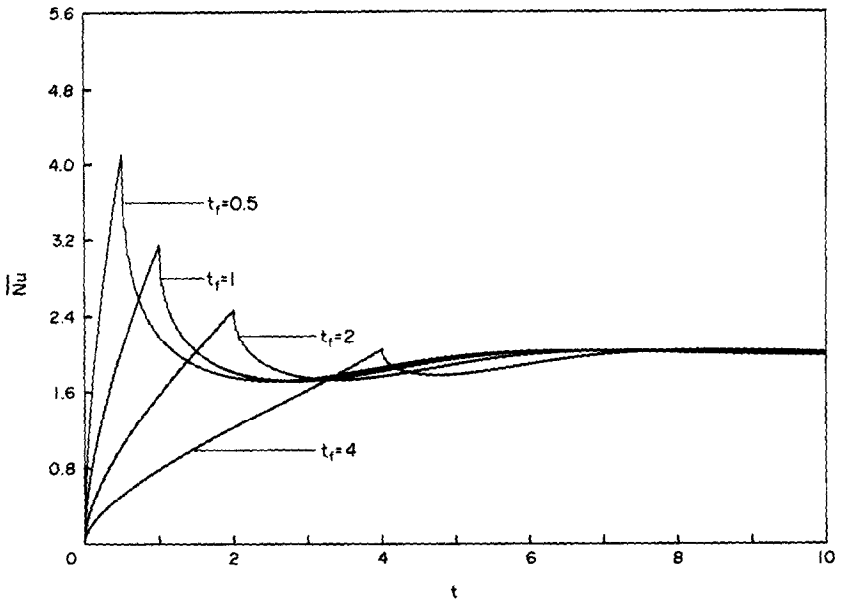

FIG. 7. Variation of average Nusselt number with time for the second mode—case of $Ra = 100$ and $t_f = 0.5$, 1.0, 2.0 and 4.0.

perature increase [$t_f = 0.5, 1.0, 2.0$ and 4.0]. Figure 7 shows the maximum value of $\overline{Nu}$ to occur at $t = t_f$ at which there is a discontinuity in the value of $\partial\phi/\partial t$. Immediately following that time, a sharp decay occurs in $\overline{Nu}$ similar to that found in the first mode. The overshoot of $\overline{Nu}$, below its final steady value, is clearly shown for all heating rates considered with approximately the same degree but takes place at different times as expected. The final steady value of $\overline{Nu}$ is found to be the same in all cases. Figure 8 shows the maximum value of $\overline{Nu}$ to occur at $t < t_f$ when $t_f = 0.5$, 1.0 and 2.0, however, for the case $t_f = 4.0$ the value of $\overline{Nu}$ reached a peak which is less than its final steady value. The variation of $\overline{Nu}$ in this mode is smooth, contrary to the first and second modes. A comparison between the variation of $\overline{Nu}$ during the transient phase for the three modes is shown in Fig. 9 for $Ra = 500$ [$t_f = 1.0$ in the second and third modes].

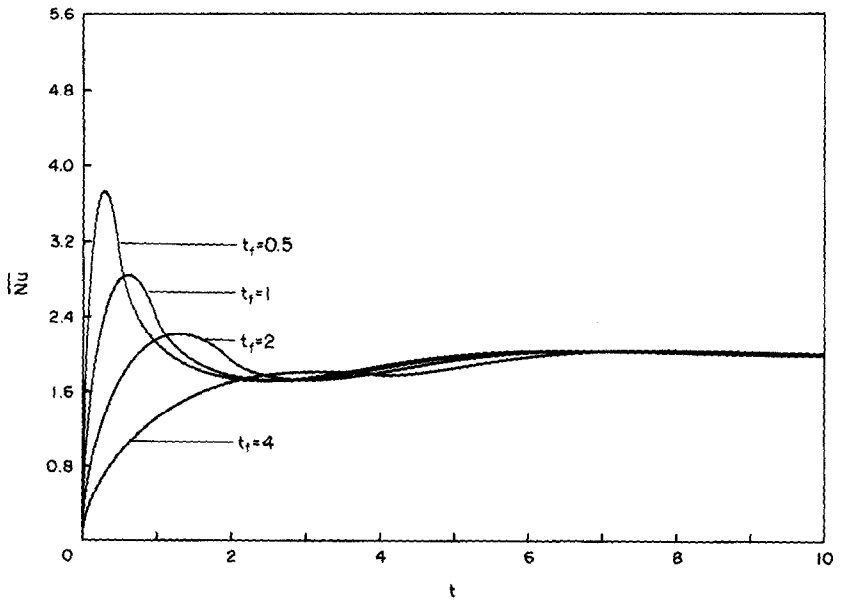

FIG. 8. Variation of average Nusselt number with time for the third mode—case of $Ra = 100$ and $t_f = 0.5$, 1.0, 2.0 and 4.0.

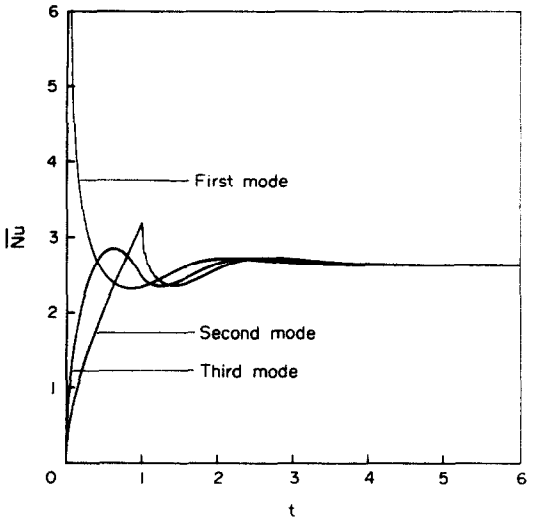

FIG. 9. Comparison between the transient behaviour of $\overline{Nu}$ for the three modes of heating for the case of $Ra = 500$ [$t_f = 1.0$ for the second and third modes].

The time development of the local Nusselt number and vorticity distributions at the rod surface are shown in Figs. 10(a) and (b), respectively, for the first mode of heating when $Ra = 300$. As can be seen in Fig. 10(a), the maximum rate of local heat transfer occurs at the bottom of the rod ($\theta = 180°$) while the minimum value occurs at the top ($\theta = 0$) at all times. It is also clear that following $t = 6$ there is no further change in the Nu distribution since the thermal field near the rod reaches, by that time, steady conditions. Figure 10(b) shows a maximum vorticity near ($\theta = 90°$) and ζ is always positive indicating no flow separation. The same criterion was also found at higher Ra values.

The variation of the velocity vector field following a sudden temperature rise is shown in Fig. 11 for the case of $Ra = 100$. At small times ($t = 0.5$, 1.0) the convective motion is sensible only in the neighbourhood of the rod near $\theta = 90°$ while the fluid at the top and bottom of the rod is almost stagnant. As time reaches $t = 2.0$, the velocity increases at the sides of the rod as well as at the top and bottom signalling the beginning of an effective convective motion. This time coincides with the time of overshoot of Nu as can been seen in Fig. 6. At $t = 4.0$, the fluid velocity at the top increases considerably and the fluid motion in the entire field becomes more developed.

The distribution of the radial and angular velocity components at $\theta = 90°$ are shown in Figs. 12(a) and (b), respectively, for the case of $Ra = 100$ at various times following a sudden temperature increase. Figure 12(a) shows negative values of v_r which means that the flow is directed towards the rod, however the non-zero value of v_θ as shown in Fig. 12(b) suggests that the flow is not exactly in the radial direction even at a large distance from the rod. Figure 12(b) also shows that an overshoot of v_θ occurs at $t = 6$. Moreover, the velocity distribution at the immediate neighbourhood of the rod reaches its final steady condition much faster than the region far away from it. The same phenomenon occurred at higher values of Ra, however, the overshoot of v_θ occurred earlier. The radial velocity distribution along the centre of the plume ($\theta = 0$) following a sudden temperature increase is shown in Fig. 13 for the same case. The

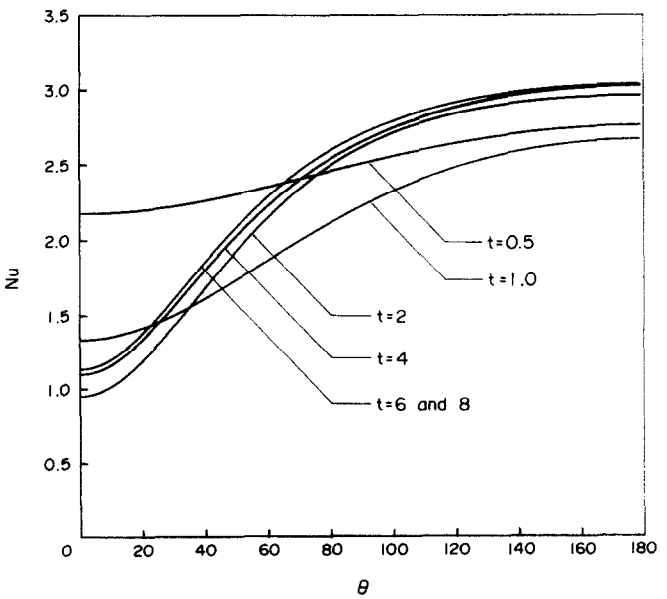

FIG. 10(a). The variation of the local Nusselt number distribution for the first mode of heating—case of $Ra = 300$.

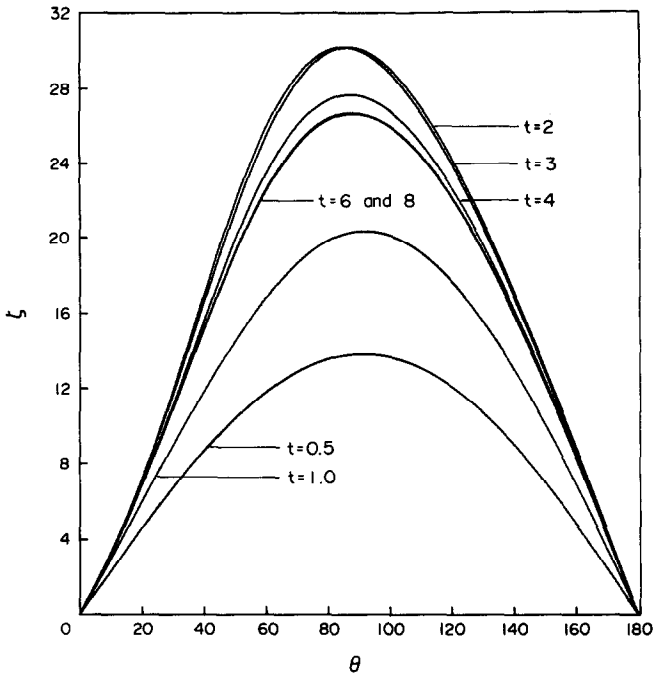

FIG. 10(b). The variation of the vorticity distribution on the rod surface for the first mode of heating—case of $Ra = 300$.

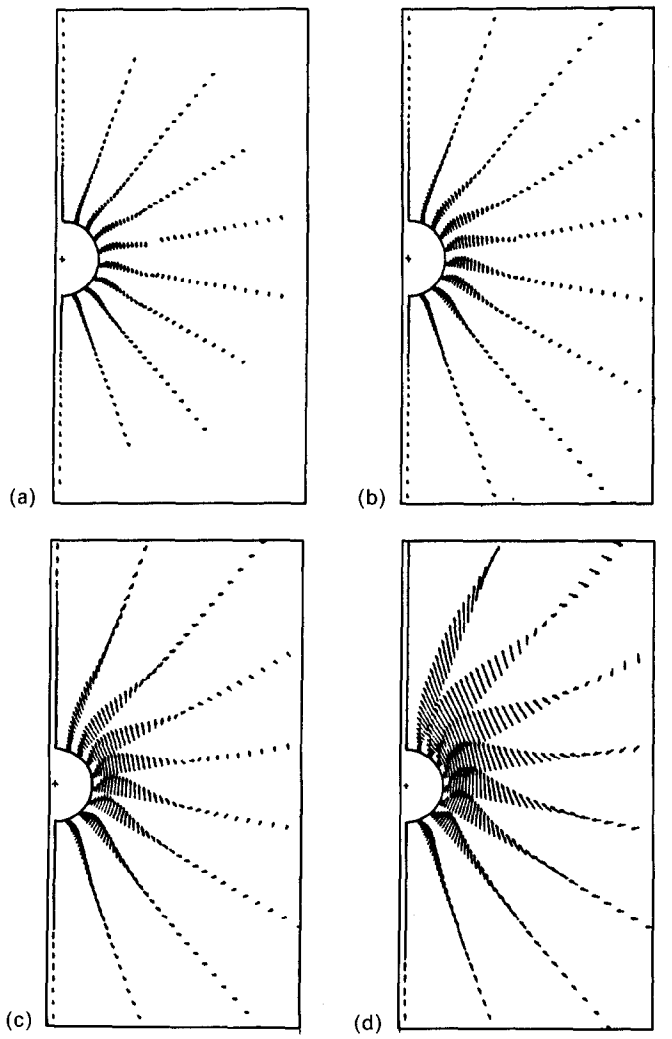

FIG. 11. The velocity vector field for the case of $Ra = 100$ and the first mode of heating: (a) $t = 0.5$; (b) $t = 1.0$; (c) $t = 2.0$; (d) $t = 4.0$.

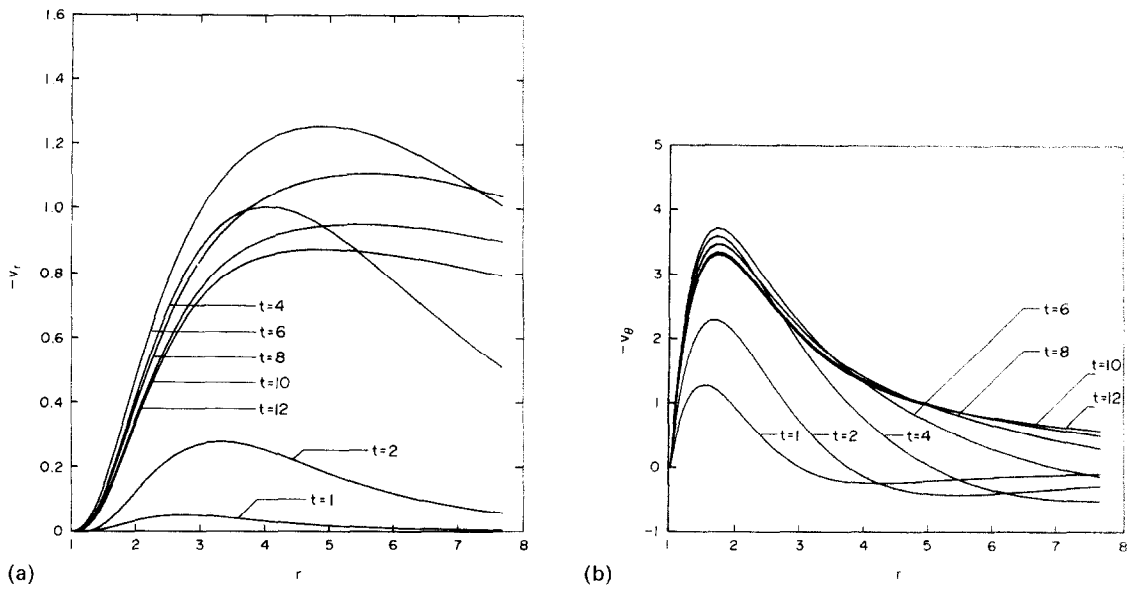

FIG. 12. Time variation of the radial and angular velocity components with r at $\theta = 90^\circ$ for the case of $Ra = 100$ and the first mode of heating: (a) radial velocity; (b) angular velocity.

maximum radial velocity adjacent to the rod surface occurred at $t = 6$ which is approximately the same time at which v_θ was maximum at $\theta = 90^\circ$. It seems that the overshoot in the upward velocity occurs in the entire field at the same time which is different from that at which the heat transfer overshoot takes place.

The temperature variation at the centre of the plume is shown in Fig. 14 at different times. The figure shows that the thickness of the thermal layer is small at small times and increases significantly as t increases.

An overshoot in the temperature gradient at the surface is clearly shown. Figures 15 and 16 show the time development of streamline and isotherm patterns following a sudden temperature rise for the cases of $Ra = 100$ and 500. Since the velocity and thermal fields are symmetric about $\theta = 0$, only one half of the field is shown. At small times, the isotherms are almost concentric circles around the rod, confirming that the initial phase of heat transfers is solely by conduction with no convection effects. This is also clearly shown in Fig. 6 where the value of $\overline{Nu}$ at small time is independent of Ra as in the case of a transient conduction regime. As time increases, the isotherms move upward at the top of the rod (region of the plume) while continue adhering to it at the bottom. The streamline patterns plotted in the same figures show that at small

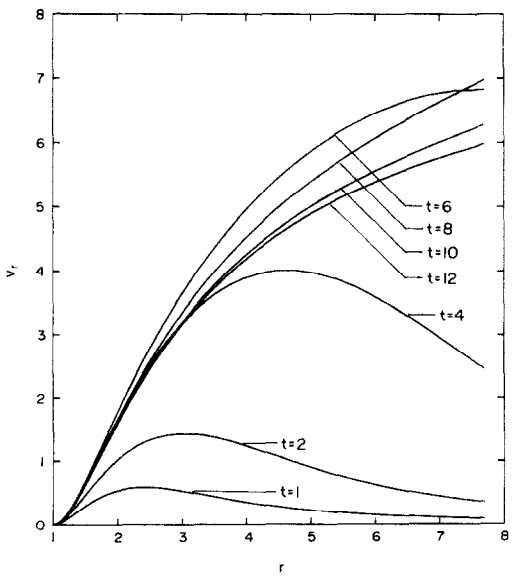

FIG. 13. Time development of the radial velocity distribution at $\theta = 0$ for the case of $Ra = 100$ and the first mode of heating.

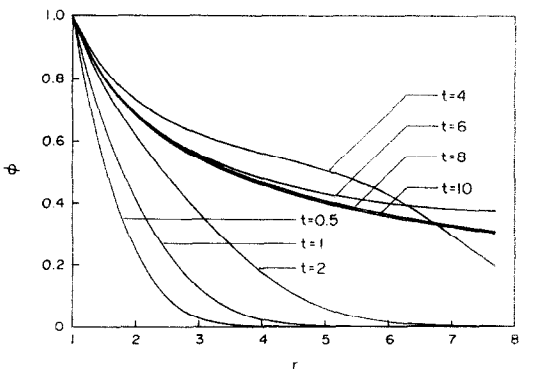

FIG. 14. The temperature distribution at $\theta = 0$ at different times following a sudden temperature rise—case of $Ra = 100$.

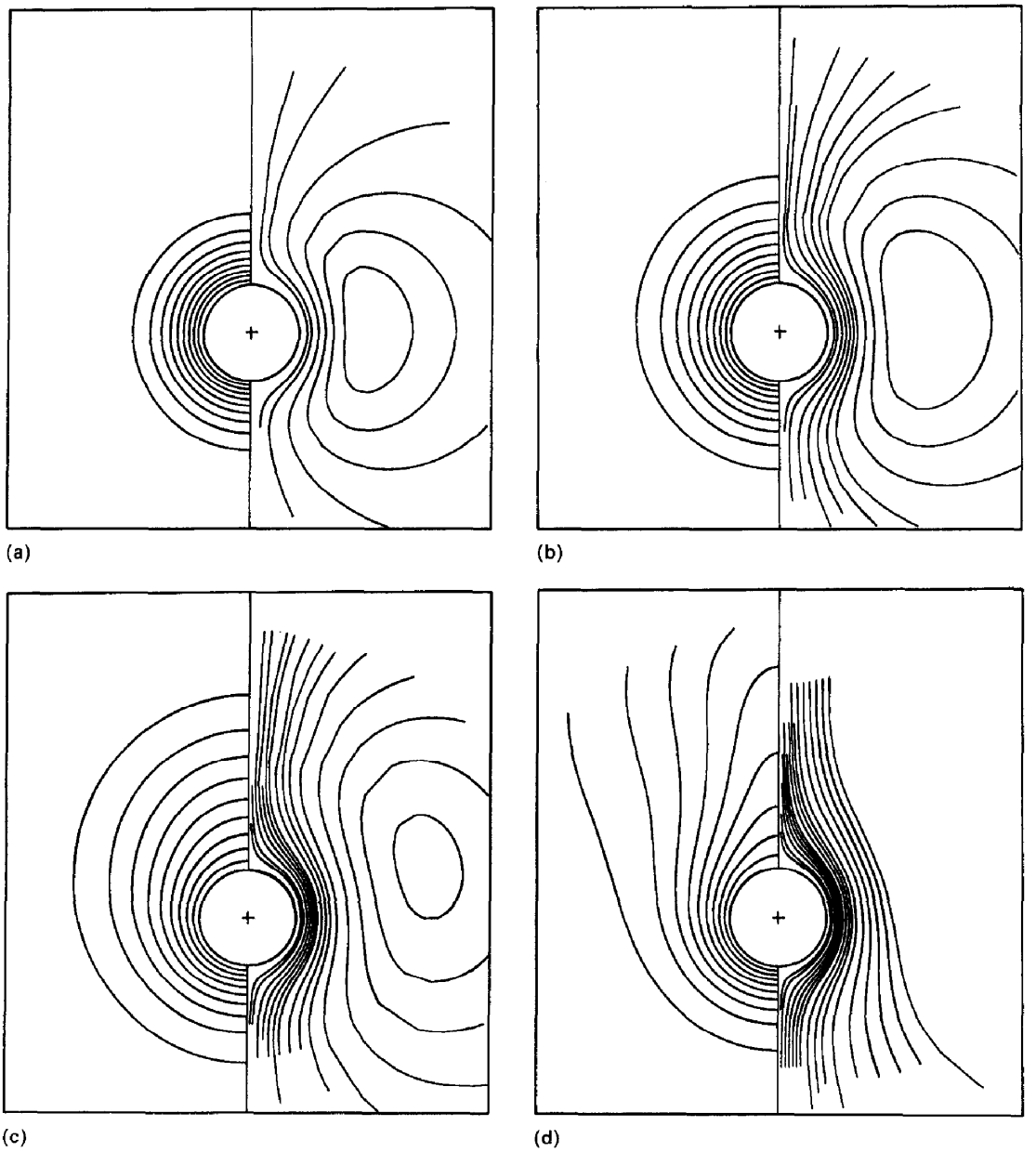

FIG. 15. The time development of the streamline and isotherm patterns for the case of $Ra = 100$ and sudden temperature rise: (a) $t = 0.5$; (b) $t = 1.0$; (c) $t = 2.0$; (d) $t = 4.0$; (e) $t = 6.0$; (f) $t = 8.0$; (g) $t = 10.0$. Streamlines plotted are $\psi = 0.05, 0.1, 0.2, 0.3, 0.4, 0.5, 0.6, 0.8, 1.0, 1.2, 1.5, 2.0, 2.5, 3.0, 3.5, 4.0$ and the isotherms plotted are $\phi = 0.1, 0.2, \ldots, 0.9$.

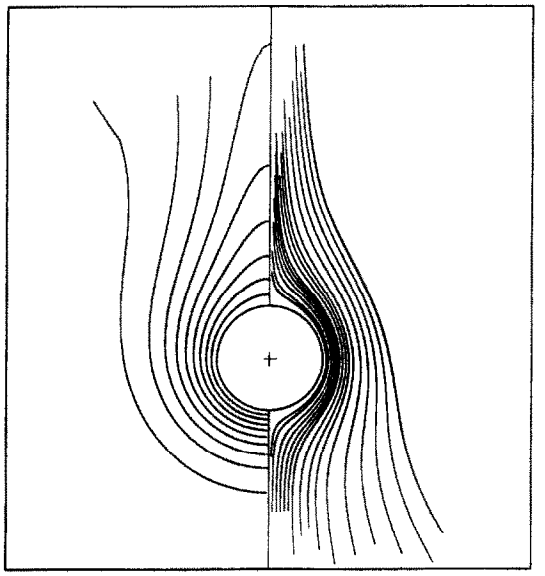

(e)

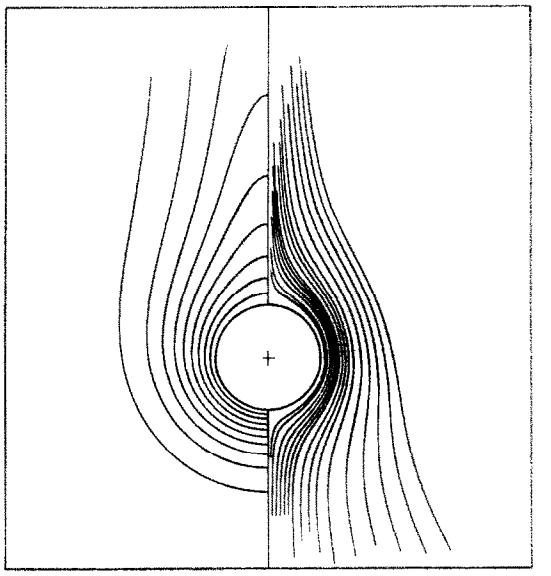

(f)

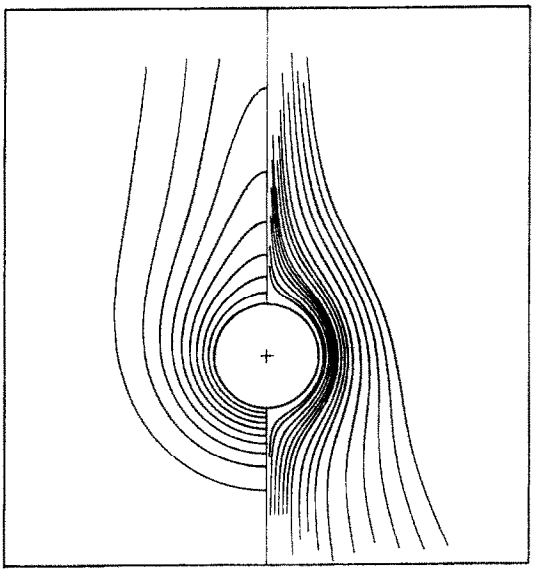

(g)

Figs. 15(e)–(g).

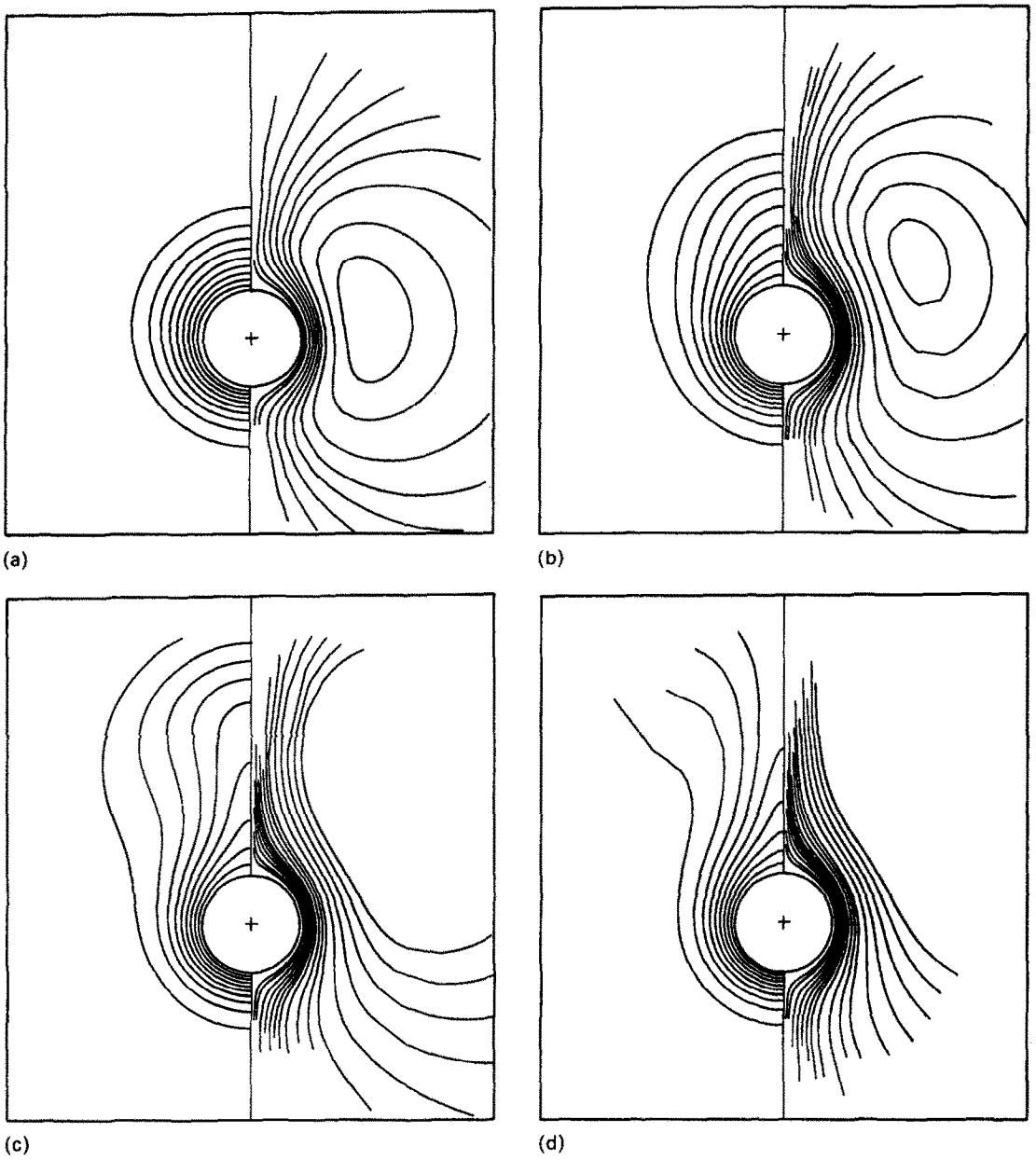

Fig. 16. The time development of the streamline and isotherm patterns for the case of $Ra = 500$ and sudden temperature rise: (a) $t = 0.5$; (b) $t = 1.0$; (c) $t = 1.5$; (d) $t = 2.0$; (e) $t = 3.0$; (f) $t = 4.0$; (g) $t = 6.0$. Streamlines plotted are $\psi = 0.1, 0.2, 0.4, 0.6, 0.8, 1.0, 1.2, 1.5, 2.0, 2.5, 3.0, 4.0, 5.0, 6.0, 7.0, 8.0$ and the isotherms plotted are the same as in Fig. 15.

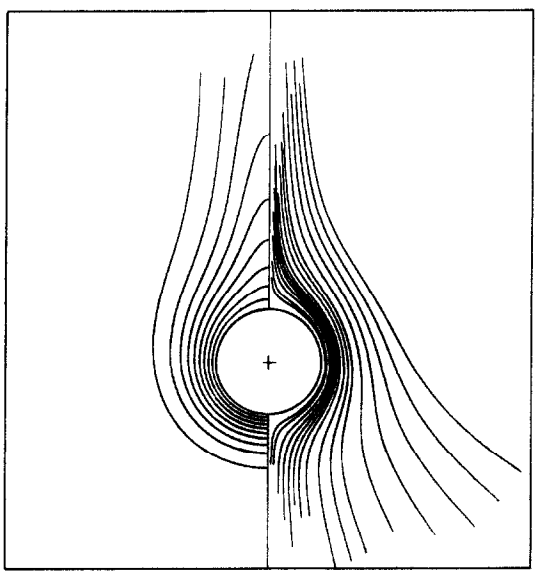

(e)

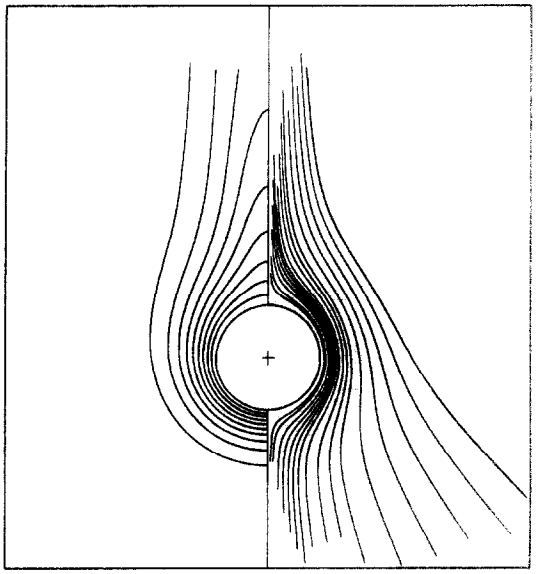

(f)

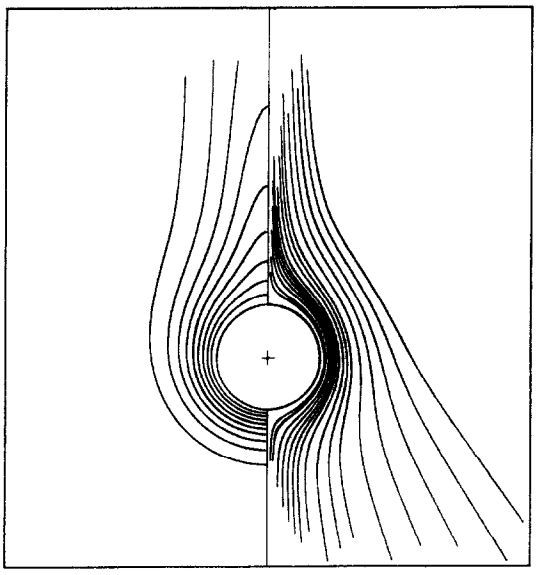

(g)

Figs. 16(e)–(g).

times the upward motion of the fluid layer near the rod surface tends to the formation of a circulating flow region on each side of the rod. The size of these regions grows with time until eventually reaching the steady pattern at which the fluid approaches the rod surface only from below.

CONCLUSION

The problem of transient buoyancy driven flow near a horizontal rod is studied for the case of two-dimensional laminar flow in the range of Rayleigh number of $10 < Ra < 1000$. Three essential modes of heating are considered. In the first one the rod surface temperature increases suddenly while the temperature increase in the second and third modes is gradual according to a certain specified form. The method of solution was verified by comparing the final steady values of the average Nusselt number as well as the local Nusselt number distribution with the available theoretical and experimental data. The agreement is found to be satisfactory. The variations of the local and average heat transfer coefficients for various heating modes are presented. The variation of the velocity distribution at various sections with time are also presented together with the streamlines and isotherms during the transient phase. The method used is not only suitable to provide solutions for the modes of heating considered in this work but can be applied also to any other mode of heating or cooling. Higher values of *Ra* are not considered here because of the excessive increase in computer time.

Acknowledgement—The author acknowledges the support received from the University of Petroleum and Minerals during this study. Assistance with plotting routines by Messrs S. M. Ahmed and M. S. Siddiqui is also acknowledged.

REFERENCES

1. R. J. Goldstein and D. G. Briggs, Transient free convection about vertical plates and cylinders, *Trans. Am. Soc. Mech. Engrs, J. Heat Transfer* **86C,** 490–500 (1964).
2. N. Brown and N. Riley, Flow past a suddenly heated vertical plate, *J. Fluid Mech.* **59,** 225–237 (1973).
3. B. Sammakia, B. Gebhart and Z. H. Qureshi, Measurements and calculations of transient natural convection in water, *Trans. Am. Soc. Mech. Engrs, J. Heat Transfer* **104,** 644–648 (1982).
4. Y. Jaluria, *Natural Convection Heat and Mass Transfer*, 1st Edn. Pergamon Press, Oxford (1980).
5. J. H. Merkin, Free convection boundary layer on an isothermal horizontal cylinder, ASME Paper No. 76-HT-16 (1976).
6. J. H. Merkin, Free convection boundary layers on cylinders of elliptic cross section, *Trans. Am. Soc. Mech. Engrs, J. Heat Transfer* **99,** 453–457 (1977).
7. T. H. Kuehn and R. J. Goldstein, Numerical solution to the Navier–Stokes equations for laminar natural convection about a horizontal isothermal circular cylinder, *Int. J. Heat Mass Transfer* **23,** 971–979 (1980).
8. B. Farouk and S. I. Guceri, Natural convection from a horizontal cylinder—laminar regime, *Trans. Am. Soc. Mech. Engrs, J. Heat Transfer* **103,** 522–527 (1981).
9. L. Elliott, Free convection on a two dimensional or axisymmetric body, *Q. J. Mech. Appl. Math.* **23,** 153–162 (1970).
10. A. S. Gupta and I. Pop, Effects of curvature on unsteady free convection past a circular cylinder, *Physics Fluids* **20,** 162–163 (1977).
11. D. B. Ingham, Free-convection boundary layer on an isothermal horizontal cylinder, *J. Appl. Mech. Phys.* **29,** 871–883 (1978).
12. G. A. Ostroumov, Unsteady heat convection near a horizontal cylinder, *J. Tech. Phys., USSR* **1,** 2627–2641 (1956).
13. L. Pera and B. Gebhart, Experimental observations of wake formation over cylindrical surfaces in natural convection flows, *Int. J. Heat Mass Transfer* **15,** 175–177 (1972).
14. C. M. Vest and M. L. Lawson, Onset of convection near a suddenly heated horizontal wire, *Int. J. Heat Mass Transfer* **15,** 1281–1283 (1972).
15. J. R. Parsons, Jr. and J. C. Mulligan, Transient free convection from a suddenly heated horizontal wire, *Trans. Am. Soc. Mech. Engrs, J. Heat Transfer* **100,** 423–428 (1978).
16. J. R. Parsons, Jr. and J. C. Mulligan, Onset of natural convection from a suddenly heated horizontal cylinder, *Trans. Am. Soc. Mech. Engrs, J. Heat Transfer* **102,** 636–639 (1980).
17. R. E. Faw, R. P. H. Ismuntoyo and T. W. Lester, Transition from conduction to convection around a horizontal cylinder experiencing a ramp excursion in internal heat generation, *Int. J. Heat Mass Transfer* **27,** 1087–1097 (1984).
18. W. M. Collins and S. C. R. Dennis, Flow past an impulsively started circular cylinder, *J. Fluid Mech.* **60,** 105–127 (1973).
19. H. M. Badr and S. C. R. Dennis, Time-dependent viscous flow past an impulsively started rotating and translating circular cylinder, *J. Fluid Mech.* **158,** 447–486 (1985).
20. H. M. Badr, Laminar combined convection from a horizontal cylinder—parallel and contra flow regimes, *Int. J. Heat Mass Transfer* **27,** 15–27 (1984).
21. B. G. Vander Hegge Zijnen, Modified correlation formula for the heat transfer by natural and forced convection from horizontal cylinders, *Appl. Scient. Res.* **A6,** 129–140 (1957).
22. M. Mikheyev, *Fundamentals of Heat Transfer*. Peace, Moscow (1956).
23. T. Tsubouchi and H. Masuda, Heat transfer by natural convection from horizontal cylinders at low Rayleigh numbers, Report of the Institute of High Speed Mechanics, Tohoku University, Vol. 19, pp. 205–219 (1967–1968).
24. H. S. Carslaw and J. C. Jaeger, *Conduction of Heat in Solids*, 2nd Edn. Oxford University Press, Oxford (1971).

TRANSFERT THERMIQUE EN CONVECTION NATURELLE VARIABLE AUTOUR D'UNE TIGE HORIZONTALE

Résumé—On étudie le transfert thermique en convection naturelle variable au voisinage d'un cylindre horizontal. La tige qui est placée dans un fluide de Boussinesq au repos et illimité est chauffée soit brusquement soit graduellement jusqu'à une température de surface constante. L'étude est basée sur la résolution des équations bidimensionnelles des bilans de masse, de quantité de mouvement et d'énergie dans le domaine de nombre de Rayleigh $10 < Ra < 1000$ en gardant constant le nombre de Prandtl à $Pr = 0{,}7$. Des résultats sont présentés pour les nombres de Nusselt variables locaux ou globaux, avec quelques détails sur les champs variables de température et de vitesse. De façon à valider la méthode de résolution employée, les valeurs stationnaires des nombres de Nusselt sont calculées et comparées avec des résultats expérimentaux et théoriques connus. Cette comparaison montre un accord satisfaisant.

WÄRMEÜBERGANG BEI INSTATIONÄRER AUFTRIEBSSTRÖMUNG UM EINEN HORIZONTALEN ZYLINDER

Zusammenfassung—Der Wärmeübergang bei instationärer Auftriebsströmung um einen horizontalen Kreiszylinder wird untersucht. Der Zylinder, der sich in einem unendlichen, ruhenden Boussinesq-Fluid befindet, wird entweder plötzlich oder langsam auf eine konstante Oberflächentemperatur aufgeheizt. Die Untersuchung wird mit Hilfe der Lösung der instationären, zweidimensionalen Bilanzgleichungen für Masse, Energie und Impuls durchgeführt. Die Rayleigh-Zahl betrug dabei zwischen 10 und 1000, die Prandtl-Zahl war konstant $Pr = 0{,}7$. Die örtliche und die mittlere instationäre Nusselt-Zahl wird als Funktion der Zeit dargestellt, daneben auch Einzelheiten des Temperatur- und Geschwindigkeits-Feldes. Um die Methode zu überprüfen, wurden auch die stationären Werte der örtlichen und mittleren Nusselt-Zahl berechnet und mit bekannten experimentellen und theoretischen Ergebnissen verglichen. Die Übereinstimmung ist zufriedenstellend.

ТЕПЛООБМЕН ПРИ НЕСТАЦИОНАРНОМ ЕСТЕСТВЕННО-КОНВЕКТИВНОМ ТЕЧЕНИИ ВОЗЛЕ ГОРИЗОНТАЛЬНОГО СТЕРЖНЯ

Аннотация—Стержень, помещенный в неподвижную неограниченную жидкость, внезапно или постепенно нагревался до постоянной температуры поверхности. Решались нестационарные двумерные уравнения сохранения массы, количества движения и энергии в приближении Буссинеска в диапазоне чисел Рэлея $10 < Ra < 1000$ при постоянном числе Прандтля $Pr = 0{,}7$. Представлены результаты для нестационарных локальных и средних чисел Нуссельта, а также некоторые данные для нестационарных полей температуры и скорости. Для подтверждения правильности выбора используемого метода решения были рассчитаны стационарные значения средних и локальных чисел Нуссельта, которые хорошо согласуются с известными экспериментальными и теоретическими данными.